Slow magnetic relaxation in dinuclear dysprosium and holmium phenoxide bridged complexes: a Dy_2 single molecule magnet with a high energy barrier.

Matilde Fondo,[a] Julio Corredoira-Vázquez,[a] Ana M. García-Deibe,[a] Jesús Sanmartín-Matalobos,[a] Silvia Gómez-Coca,[b] Eliseo Ruiz[b], Enrique Colacio[c]*

[a] Departamento de Química Inorgánica, Facultade de Química, Universidade de Santiago de Compostela, Campus Vida, 15782 Santiago de Compostela, Spain.

[b] *Departament de Química Inorgànica i Orgànica, and Institut de Química Teórica i Computacional, Universitat de Barcelona, 08028 Barcelona, Spain*

[c] *Departamento de Química Inorgánica, Facultad de Ciencias, Universidad de Granada, Avda Fuentenueva s/n, 18071 Granada, Spain*

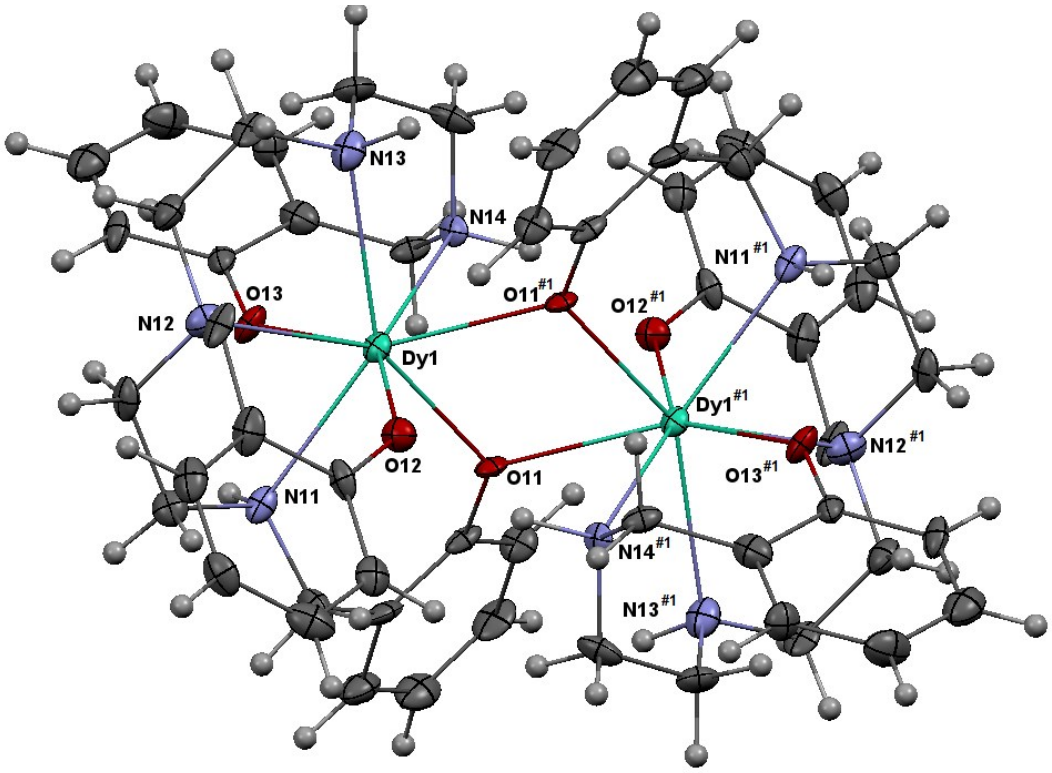

Figure S1. Ellipsoid (50% probability) diagram for $\mathbf{Dy_2}$ (from $\mathbf{Dy_2}$·2THF)

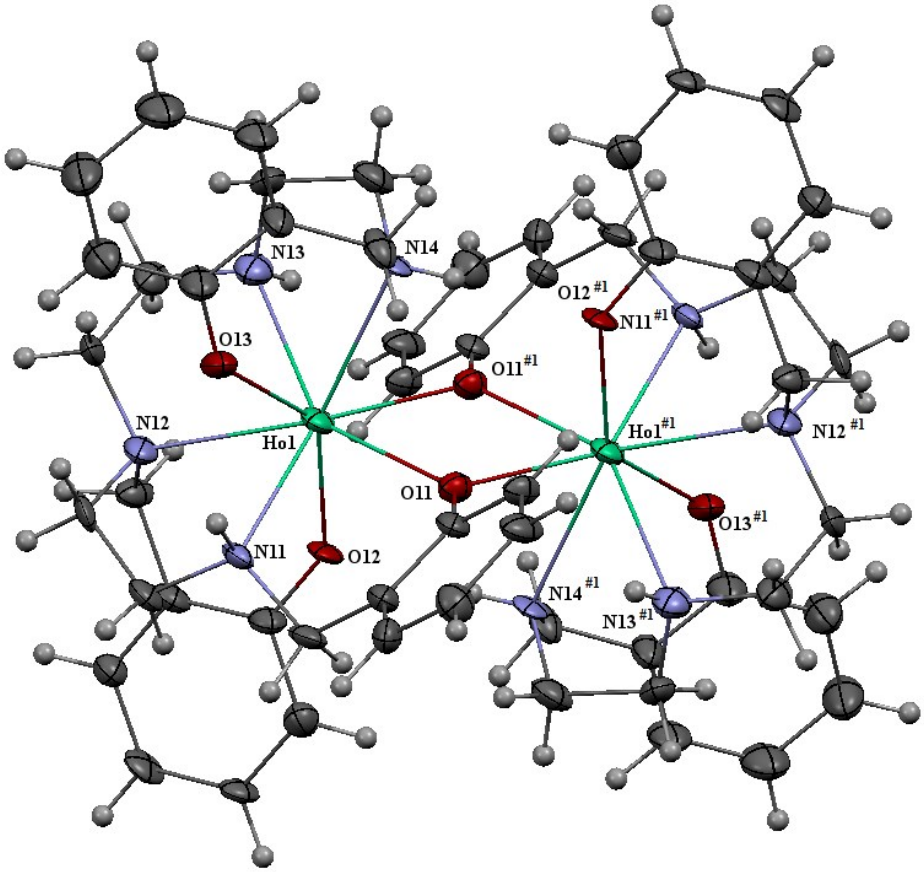

Figure S2. Ellipsoid (50% probability) diagram for $\mathbf{Ho_2}$.

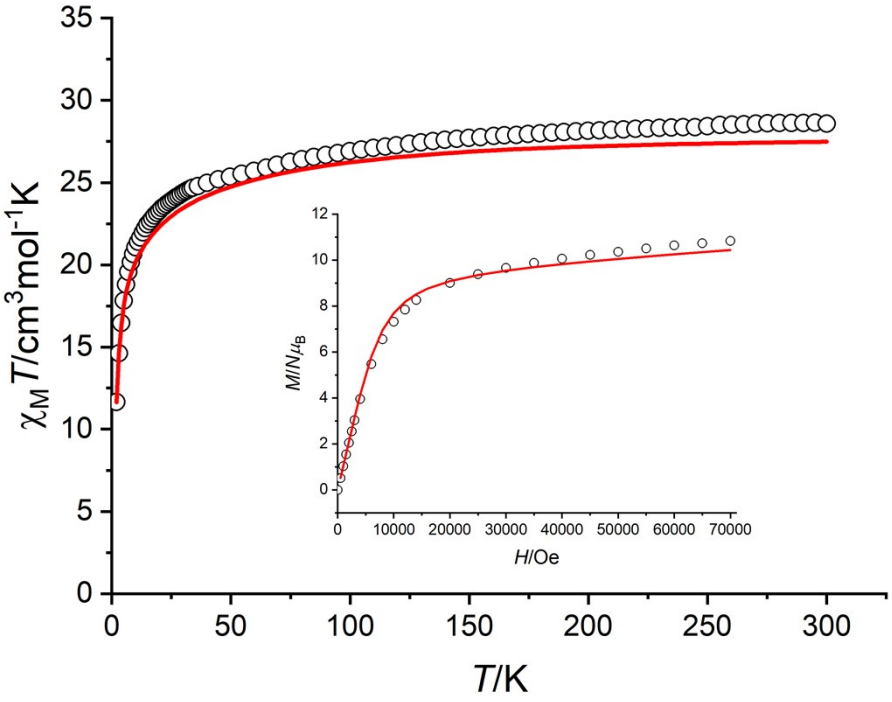

Figure S3. $\chi_M T$ *vs T* for **Ho_2**. Inset: $M/N\mu_B$ *vs H*. The solid red lines represent the theoretical data obtained from *ab inito* calculations including the dipolar interactions

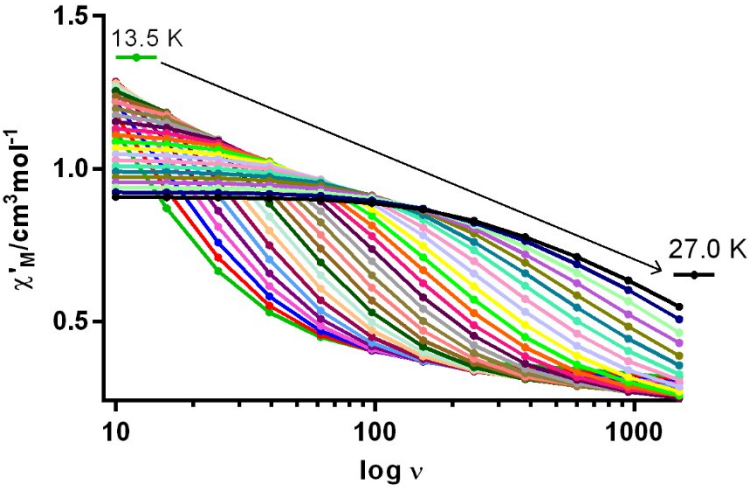

Figure S4. Frequency dependence of χ'_M for **Dy_2** in a zero dc field at different temperatures.

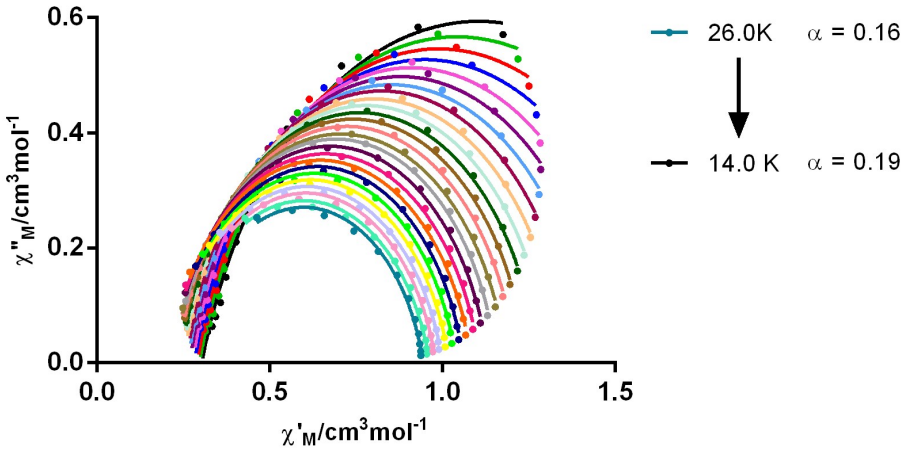

Figure S5. Cole-Cole plot for **Dy_2** at zero dc field.

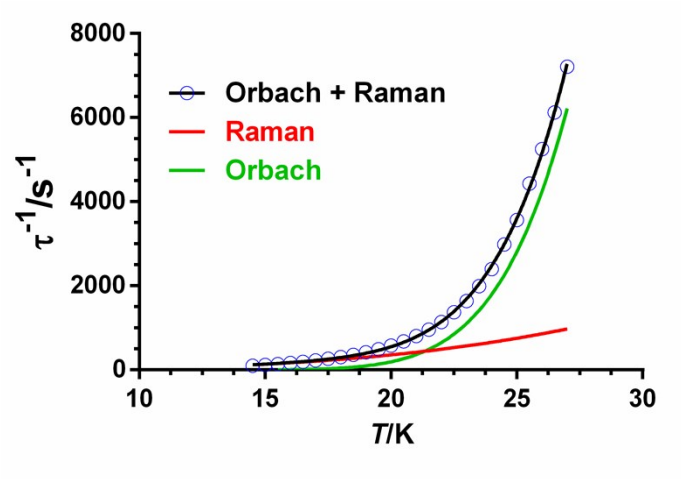

Figure S6. Arrhenius plot for **Dy_2** in a zero dc field showing the Raman, Orbach and combination of Raman-Orbach fits.

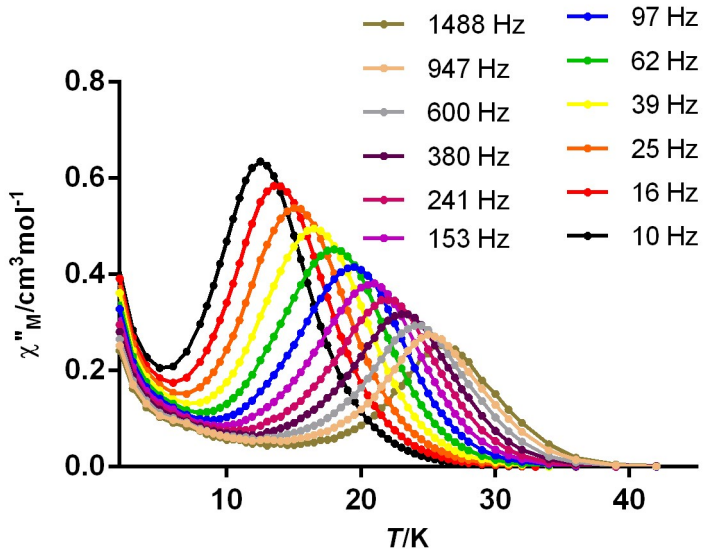

Figure S7. Temperature dependence of χ''_M for **Dy_2** in a zero dc field at different frequencies.

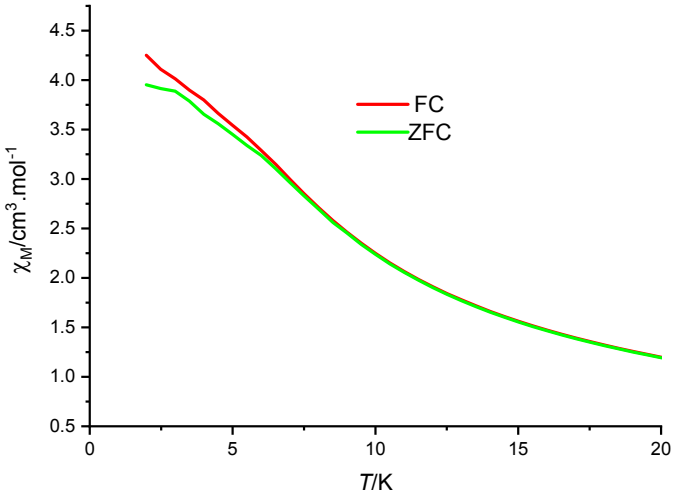

Figure S8. Field-cooled (FC) and zero-field-cooled (ZFC) magnetization for **Dy_2**, measured under a 1000 Oe dc field in warm mode (2 K/min).

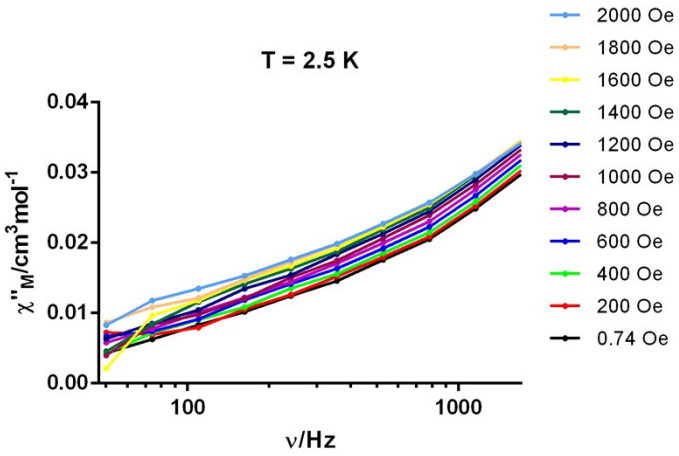

Figure S9. Frequency dependence of χ''_M for **Ho_2**·$4H_2O$ at 2.5 K under different magnetic fields.

Dy_2·Py1 **Dy_2·Py2**

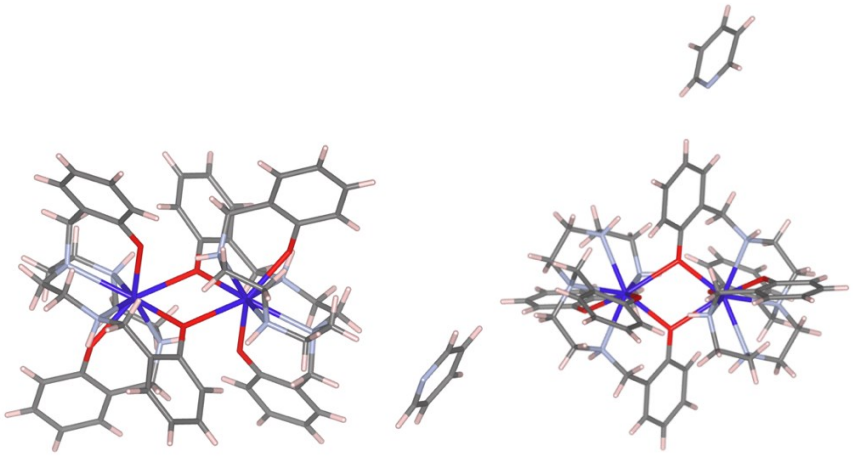

Figure S10. Employed geometry for the Dy_2 molecules including the Py molecule.

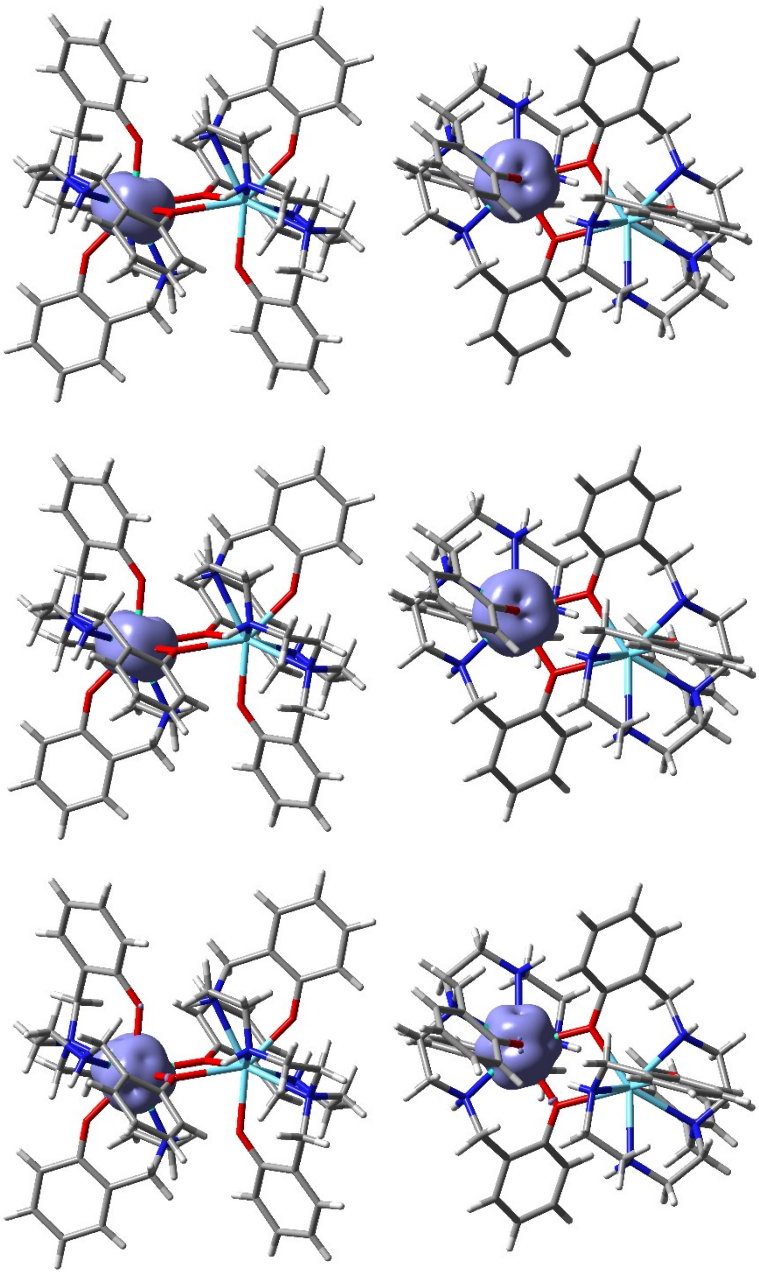

Figure S11. Isosurface of the CASSCF beta electron density of one of the Dy^{III} ions of $\mathbf{Dy_2}$ calculated as the difference between the total density and the spin density of the seven alpha active electrons. It is shown for the ground (above), first excited (middle) and second excited (below) states.

Table S1. Main bond distances (Å) and angles (º) for **Dy_2**·2THF**, Dy_2**·2Py and **Ho_2**·2Py

	Dy_2·2THF	**Dy_2**·2Py	**Ho_2**·2Py
M1-O13	2.261(7)	2.261(10)	2.241(8)
M1-O12	2.264(7)	2.254(9)	2.271(7)
M1-O11	2.319(7)	2.340(8)	2.318(7)
M1-O11$^{\#1}$	2.481(7)	2.512(10)	2.487(7)
M1-N12	2.590(10)	2.591(10)	2.561(9)
M1-N11	2.503(9)	2.522(10)	2.511(8)
M1-N13	2.586(9)	2.579(10)	2.567(9)
M1-N14	2.560(8)	2.529(9)	2.520(8)
M1···M1#1	3.9219(12)	3.945(7)	3.9332(12)
M1-O11-M1$^{\#1}$	109.5(3)	108.7(3)	109.9(3)
O12-M1-N14	149.2(3)	149.6(3)	149.5(3)
O13-M1-N11	66.5(3)	66.3(3)	66.2(3)

$^{\#1}$ -x+1,-y+1,-z

Table S2. SHAPE v2.1. Continuous shape measures calculation (c) 2013 Electronic Structure Group, Universitat de Barcelona.

Geometries Coordination number 8

ETBPY-8	13 D3h	Elongated trigonal bipyramid
TT-8	12 Td	Triakis tetrahedron
JSD-8	11 D2d	Snub diphenoid J84
BTPR-8	10 C2v	Biaugmented trigonal prism
JBTPR-8	9 C2v	Biaugmented trigonal prism J50
JETBPY-8	8 D3h	Johnson elongated triangular bipyramid J14
JGBF-8	7 D2d	Johnson gyrobifastigium J26
TDD-8	6 D2d	Triangular dodecahedron
SAPR-8	5 D4d	Square antiprism
CU-8	4 Oh	Cube
HBPY-8	3 D6h	Hexagonal bipyramid
HPY-8	2 C7v	Heptagonal pyramid
OP-8	1 D8h	Octagon

$[Dy(H_3L^{1,2,4})]_2 \cdot 2THF$ (**Dy_2**$\cdot 2THF$)

Structure [ML8]	ETBPY-8	TT-8	JSD-8	BTPR-8	JBTPR-8	JETBPY-8
	22.932,	10.574,	2.469,	1.849,	2.092,	27.040
JGBF-8	**TDD-8**	**SAPR-8**	CU-8	HBPY-8	HPY-8	OP-8
11.890,	**1.073**,	**1.711**,	10.216,	16.903,	23.858,	27.986

$[Dy(H_3L^{1,2,4})]_2 \cdot 2Py$ (**Dy_2**$\cdot 2Py$)

Structure [ML8]	ETBPY-8	TT-8	JSD-8	BTPR-8	JBTPR-8	JETBPY-8
	23.149,	10.665,	2.554,	1.844,	2.126,	26.641
JGBF-8	**TDD-8**	**SAPR-8**	CU-8	HBPY-8	HPY-8	OP-8
12.006,	**1.178**,	**1.520**,	10.328,	16.912,	23.734,	27.954

$[Ho(H_3L^{1,2,4})]_2 \cdot 2Py$ (**Ho_2**$\cdot 2Py$)

Structure [ML8]	ETBPY-8	TT-8	JSD-8	BTPR-8	JBTPR-8	JETBPY-8
	22.979,	10.694,	2.655,	1.813,	2.072,	26.651,
JGBF-8	**TDD-8**	**SAPR-8**	CU-8	HBPY-8	HPY-8	OP-8
12.113,	**1.230**,	**1.478**,	10.316,	16.970,	23.459,	27.656

Table S3. Generalised Debye model fitting parameters for **Dy_2**

T/K	χ_S/(cm^{3}mol^{-1})	χ_T/(cm^{3}mol^{-1})	τ/(10^{-4}s)	α
14.0	0.30	1.91	128.0	0.19
14.5	0.30	1.79	104.7	0.17
15.0	0.29	1.69	86.7	0.16
15.5	0.28	1.62	72.9	0.15
16.0	0.28	1.54	61.7	0.13
16.5	0.27	1.49	52.4	0.13
17.0	0.26	1.44	44.8	0.12
17.5	0.26	1.39	38.1	0.11
18.0	0.25	1.35	32.8	0.11
18.5	0.25	1.31	28.0	0.11
19.0	0.24	1.28	23.9	0.11
19.5	0.24	1.24	20.4	0.11
20.0	0.23	1.21	17.4	0.11
20.5	0.22	1.19	14.7	0.12
21.0	0.23	1.16	12.5	0.11
21.5	0.22	1.13	10.5	0.12
22.0	0.21	1.11	8.8	0.13
22.5	0.21	1.09	7.3	0.14
23.0	0.21	1.06	6.1	0.14
23.5	0.21	1.04	5.0	0.14
24	0.21	1.02	4.2	0.15
24.5	0.22	1.00	3.3	0.16
25.0	0.23	0.98	2.8	0.15
25.5	0.23	0.96	2.3	0.16
26.0	0.25	0.95	1.9	0.16

Table S4. Calculated energies (in cm^{-1}) of the states before the inclusion of the spin-orbit effect.

State	Ho_2	Dy_2	Dy_2·Py1	Dy_2·Py2
1	0	0	0	0
2	47.6	5.1	4.6	4.7
3	102.0	308.1	305.3	306.1
4	159.8	365.9	352.1	354.5
5	209.9	416.5	412.2	412.6
6	251.8	460.3	452.1	454.8
7	267.2	520.7	510.9	513.8
8	327.6	569.4	577.3	577.5

Table S5. Calculated energies (in cm^{-1}) of the 8 lowest Kramers doublets after the RASSI step for the Dy_2 compounds.

KDs	Dy_2	Dy_2·Py1	Dy_2·Py2
1	0	0	0
2	231.6	230.9	231.8
3	341.9	334.6	335.9
4	405.7	395.3	396.4
5	470.1	459.7	461.2
6	517.2	507.7	510.4
7	578.4	577.6	578.0
8	750.6	751.7	751.4

Table S6. Calculated energies (in cm^{-1}) of the 17 lowest states after the RASSI step for the Ho_2 compound.

State	Ho_2
1	0
2	1.71
3	61.7
4	68.4
5	122.8
6	151.1
7	186.3
8	194.3
9	204.3
10	221.4
11	249.8
12	252.9
13	302.9
14	308.7
15	333.2
16	394.3
17	396.8

Table S7. Crystal data and structure refinement for $[Dy(H_3L^{1,2,4})]_2 \cdot 2THF$ (**Dy_2**·2THF), $[Dy(H_3L^{1,2,4})]_2 \cdot 2Py$ (**Dy_2**·2Py) and $[Ho(H_3L^{1,2,4})]_2 \cdot 2Py$ (**Ho_2**·2Py)

	Dy_2·2THF	**Dy_2**·2Py	**Ho_2**·2Py
Empirical formula	$C_{64}H_{82}Dy_2N_8O_8$	$C_{64}H_{76}Dy_2N_{10}O_6$	$C_{64}H_{76}Ho_2N_{10}O_6$
Molecular weight	1392.35	1406.34	1411.20
Crystal system	Monoclinic	Triclinic	Triclinic
Space group	$P2_1/n$	P-1	P-1
Wavelength (Å)	0.71073	0.71073	0.71073
Crystal size (mm^3)	0.070 x 0.060 x 0.020	0.740 x 0.260 x 0.080	0.070 x 0.050 x 0.020
Color, shape	Prism, colorless	Needle, colorless	Prism, colorless
T (K)	100(2)	100(2)	100(2)
a (Å)	13.480(4)	9.902(18)	9.8904(11)
b (Å)	14.259(4)	12.75(3)	12.7769(15)
c (Å)	15.403(4)	13.67(3)	13.6362(17)
α (º)	90	64.03(5)	64.096(3)
β (º)	106.770(9)	76.98(4)	76.914(4)
γ (º)	90	67.75(4)	67.662(3)
Volume ($Å^3$)	2834.7(13)	1432(5)	1430.0(3)
Z	2	2	1
Absorpt. coef. (mm^{-1})	2.680	2.651	2.809
Reflections collected	51827	18178	31962
Independent reflections	5801 [R(int) = 0.1259]	5235 [R(int) = 0.1695]	5220 [R(int) = 0.1253]
Data / restraints / param.	5801 / 6 / 361	5235 / 0 / 370	5220 / 12 / 370
Final R indices [$I>2\sigma(I)$]	R_1 = 0.0885 wR_2 = 0.2050	R_1 = 0.0711 wR_2 = 0.1486	R_1 = 0.0719 wR_2 = 0.1488
R indices (all data)	R_1 = 0.1077 wR_2 = 0.2150	R_1 = 0.1307 wR_2 = 0.1749	R_1 = 0.1017 wR_2 = 0.1638